RSC Advances

PAPER

View Article Online
View Journal | View Issue

Cite this: *RSC Adv.*, 2025, **15**, 602

Composition of the isopropanol-soluble portion and fast pyrolysis product distribution of the insoluble part from Pakistani lignite†

Gui-han Zhao,[ab] Ya-ya Ma,[a] Yuan Ren,[a] Jun Xiao,[a] Wen-Long Mo, *[ab] Jia Guo,*[b] Xian-Yong Wei,[a] Xing Fan[a] and Akram Naeem[c]

Pakistani lignite (PLC) was thermally dissolved at 300 °C using isopropanol (IPA) to obtain a soluble portion (SP) and insoluble portion (ISP). Proximate analysis, ultimate analysis, Fourier transform infrared spectrometry (FTIR), thermogravimetric analysis (TG-DTG) and pyrolysis-gas chromatography/mass spectrometry (Py-GC/MS) results were compared to explore the influence of the thermal dissolution process on the pyrolysis for PLC and ISP. Results showed that the thermal dissolution process mainly dissolved some light components of low-rank coal, and more phenols, aldehydes, esters and ethers were found in the SP, indicating that low-carbon alcohols can break the ether bridge bond in coal and generate oxygen-containing organic compounds (OCOCs). Compared with PLC, ISP had better thermal stability, low activation energy and pre-exponential factor. Furthermore, thermal dissolution dissolves small molecular compounds in coal channels, enlarges the pore structure and mass transfer rate, and enables the compounds produced in the pyrolysis process to diffuse to the surface of coal faster. On the other hand, IPA could be used as a hydrogen supply solvent to weaken the oxygen bridge bond in the macromolecular structure of coal, so that it is easier to break during pyrolysis. Thus, it was demonstrated that the low molecular weight compounds have a significant effect on the low temperature pyrolysis characteristics of PLC, and these two processes could potentially improve the added value of coal.

Received 30th October 2024
Accepted 16th December 2024

DOI: 10.1039/d4ra07749k

rsc.li/rsc-advances

1. Introduction

Pakistan is rich in coal resources. According to the estimation of the Geological Survey of Pakistan, the coal resources in Pakistan comprise about 185 billion tons,[1] mainly including low-rank coals, with great differences in its physical characteristics and chemical compositions. Pakistani coal presents high sulfur and ash contents, and its graded and high-efficiency utilization has become an essential research direction in the country.[2–4]

Thermal dissolution of coals is considered an effective method for efficiently utilizing coals.[5] It separates the soluble portion (SP) from the coal macromolecular skeleton by placing the coal sample and solvent in a reactor under an inert atmosphere, and the temperature is usually set tobelow 300 °C. Compared with extraction, an increase in temperature can reduce the viscosity and surface tension of the used solvent and an increase in pressure is conducive to bubble dissolution. It can effectively weaken and destroy the non-covalent bond interactions between organic compounds, such as hydrogen bonding, dispersion force, and dipole moment, so that the SP can be completely dissolved.[6] This method can be used to analyze the composition and structure characteristics of the organic compounds in coal, while keeping the main structure of coal intact as much as possible.[7] There are literature reports on separately developed "ash-free coal" and "variable temperature thermal dissolution technology" approaches. The use of inert solvents with high boiling points (such as tetrahydronaphthalene and 1-methylnaphthalene) can convert over 60% of the organic matter in low rank coal into soluble organics without using H_2 and catalysts.[8,9] However, the boiling points of these solvents are too high and the process is expensive, which is not conducive to the separation of the soluble portion and the used solvent, presenting difficulties for the analysis and further processing and utilization of the thermal dissolution compounds.

To overcome the shortcomings of high boiling-point solvents, low boiling-point solvents that are easily recycled are increasingly being used in thermal dissolution research of coal. Commonly used thermal dissolution solvents include non-polar solvents (*n*-hexane, benzene, toluene, cyclohexane, *etc.*) and polar solvents (methanol, ethanol, isopropanol, *etc.*).[10–13] Ma

[a]*State Key Laboratory of Carbon Based Energy Resource Chemistry and Utilization, Xinjiang Key Laboratory of Clean Coal Transformation and Chemical Process, College of Chemical Engineering, Xinjiang University, Urumqi, 830017, Xinjiang, China. E-mail: mowenlong@xju.edu.cn*

[b]*Xinjiang Energy Co., LTD, Urumqi, 830000, Xinjiang, China*

[c]*School of Chemical Engineering, Minhaj University Lahore, Lahore, 54000, Punjab, Pakistan*

† Electronic supplementary information (ESI) available. See DOI: https://doi.org/10.1039/d4ra07749k

et al.[14] used petroleum ether, methanol and carbon disulfide/acetone (CS_2/AC) to extract Hefeng bituminous coal step-by-step, and the results showed that methanol presented a higher extraction rate, while CS_2/AC was more conducive to the dissolution of alcohols. Zhang *et al.*[15] used methanol, toluene, and acetone as solvents to obtain soluble oxygen-containing organic compounds from soft coal and hard coal with ultrasound, thermal dissolution, and ultra-high pressure extraction methods. It has been found that most of the oxygen atoms in oxygen-containing organic compounds in low-rank coal exist on the side chains of aromatic structures. Hu *et al.*[4] used Naomaohu lignite for sequential dissolution with cyclohexane, ethanol and isopropanol at 300 °C to affect the structure and pyrolysis characteristics of lignite. Results showed that the yield of isopropanol was the highest. Furthermore, sequential thermal dissolution is beneficial for the pyrolysis of lignite, and can break some noncovalent bonds and weaken covalent bonds. As mentioned above, the yield of soluble organic matter in polar solvents is relatively higher than that in non-polar solvents.

Mild thermal dissolution can obtain some (~40%) high value-added soluble organics from coal, while about 60% of the insoluble parts (including the macromolecular network skeleton) in coal is still not being utilized. Coal pyrolysis refers to a series of complex physical–chemical changes when coal is heated to a higher temperature under isolated air or an inert atmosphere.[16,17] Low-to-medium temperature pyrolysis can obtain high value-added tar, high calorific pyrolysis gas, and semi-coke, which is the main thermochemical conversion method for the efficient and clean utilization of medium and low rank coals.[18–25] Li *et al.*[26] first used *n*-hexane to thermally dissolve Hongliulin coal at 260–340 °C to obtain thermally soluble matter and insoluble parts at different temperatures, and used a fixed bed reactor to pyrolyze Hongliulin coal and its insoluble parts to obtain pyrolysis products. Analysis of the pyrolysis products revealed the structural and compositional characteristics of the insoluble portions, which showed that the yields of pyrolysis liquid and gaseous products from the thermal dissolution residues decreased with rising thermal dissolution temperature. Therefore, through the thermal dissolution of coal, organic chemicals with lower molecular weight can be obtained under milder conditions. Then, the thermal-dissolved residue is selectively pyrolyzed to obtain pyrolysis oil with relatively simple components through medium and low temperature pyrolysis, which can further produce clean liquid fuels with high added value through hydrogenation and other means. In general, this multistage treatment method can make comprehensive use of coal resources.

In this research, Pakistan lignite (PLC) was thermally dissolved with isopropanol at 300 °C to obtain the soluble portion (SP) and insoluble part (ISP). The characteristics of the SP composition were investigated and analyzed by GC/MS method. The basic features of PLC and ISP were characterized by proximate analysis, ultimate analysis, FTIR, and TG-DTG methods. Finally, the fast pyrolysis will be performed by Py-GC/MS at 450 °C, and the differences in the composition and products distribution will be compared to explore the influence of thermal dissolution process on the pyrolysis of coal.

2. Experiments

2.1 Materials

PLC was collected from the Dukki coal mine in Balochistan, Pakistan. In accordance with GB/T212-2008, the proximate analysis of PLC was conducted, and the results are listed in Table 1. All reagents used in the study are analytical reagents. Isopropyl alcohol (IPA) was purified by a rotary evaporator at 90 °C before use.

2.2 Experimental procedure

As shown in Fig. 1, 5 g of PLC and 20 mL of IPA were put into an autoclave equipped with a magnetic stirrer (YZPR-100-M). The autoclave was heated to 300 °C at a rate of 20 °C min^{-1} under an initial pressure of 1 MPa after purging with nitrogen 3 times, and the thermal dissolution process was maintained at that

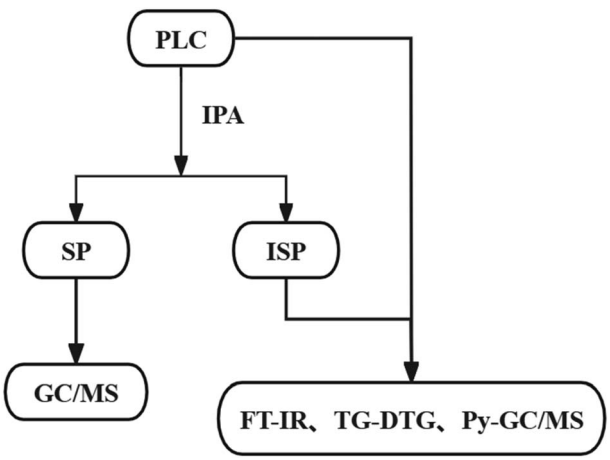

Fig. 1 Experimental method.

Table 1 Proximate and ultimate analyses of samples (wt%)[a]

	Proximate analysis				Ultimate analysis (daf)					
Sample	M_{ad}	A_d	VM_{daf}	FC_{daf}^{diff}	C	H	N	O^{diff}	$S_{t,d}$	H/C
PLC	5.92	9.29	46.69	53.31	65.93	4.11	0.79	>28.07	1.10	0.75
ISP	4.73	15.69	40.12	59.88	67.31	4.36	1.14	>23.53	3.66	0.78

[a] ad: air-dry basis; daf: dry and ash-free basis; diff: by difference.

temperature for 2 hours. After that, the products in the autoclave were taken out, and filtrated into the solid phase (SP) and liquid phase. The solid one was washed to remove some liquids in its pores with IPA as the solvent, and then the ISP was obtained.

2.3 Analytical methods

Ultimate analysis was performed using an Elemantar Vario EL cube elemental analyzer (Elementar UNICUBE, Germany), in accordance with GB/T 476-2008. The pyrolysis performances of PLC and ISP were conducted by thermogravimetric analyzer (SDTQ 600). 10 mg of sample was loaded into the ceramic crucible, and the sample was heated from room temperature to 1000 °C at the rate of 10 °C min^{-1} under a nitrogen atmosphere. Functional groups of PLC and ISP were analyzed by FTIR (Thermo Scientific Nicolet iS20) at a resolution of 4 cm^{-1}. The analysis was performed with 32 scans over a wavenumber range of 400–4000 cm^{-1}. All fitting curves in the experiments were generated using Peakfit 4 software.

The thermal dissolution products SP was analyzed using GC/MS (Agilent 7890/5795). The instrument was equipped with an HP-5MS chromatographic column, and high-purity helium gas (1 mL min^{-1}) was used as the carrier gas. The inlet temperature was set at 250 °C with a temperature program of 60 °C for 3 min, followed by a ramp rate of 10 °C min^{-1} up to 300 °C for 10 min. The split ratio was 20 : 1, and the mass scan range was set from

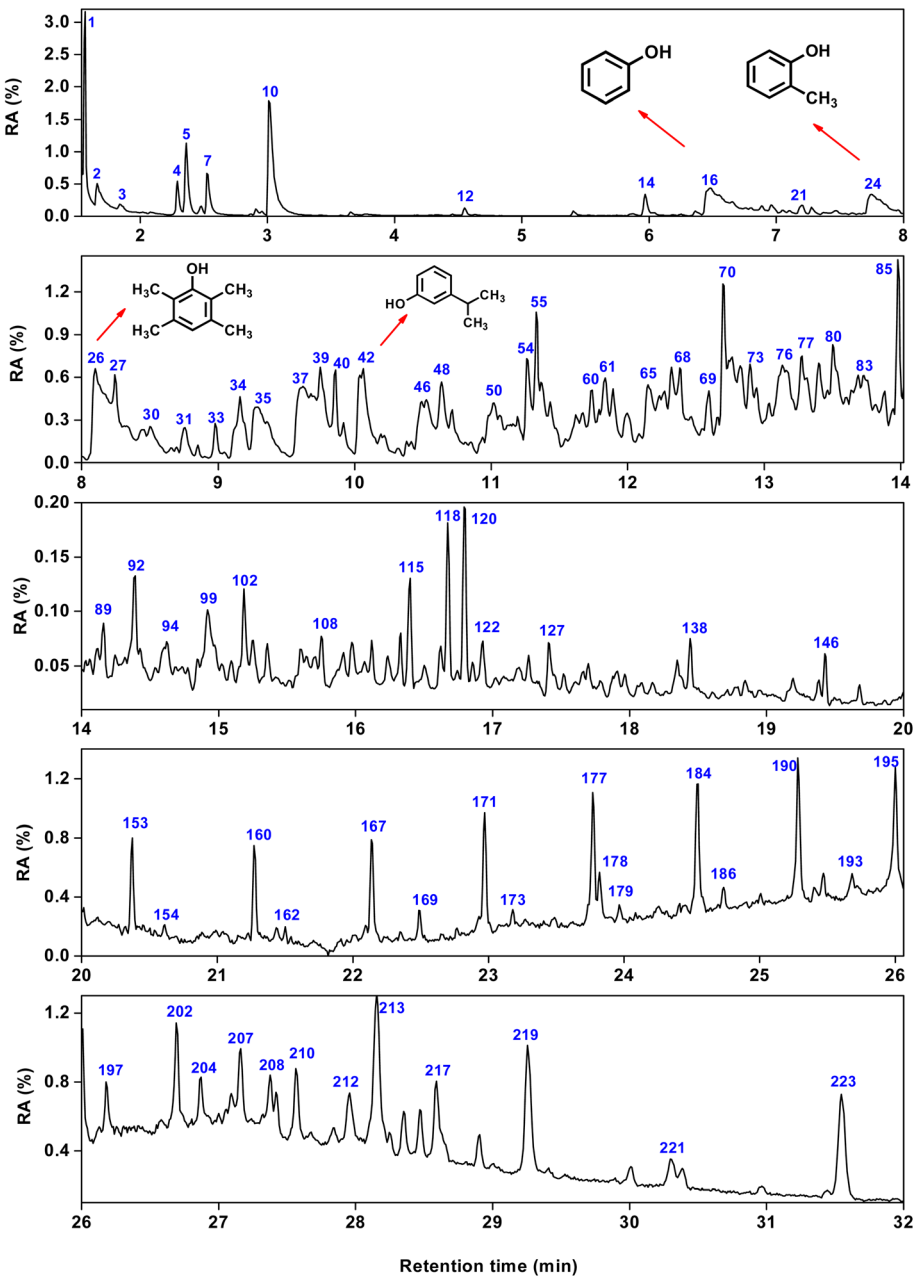

Fig. 2 Total ion chromatogram of SP.

35 to 800 μ. The fast pyrolysis experiment was performed by an EGA/PY-3030D pyrolyzer, and the volatile characteristic components of PLC and ISP were analyzed qualitatively and quantitatively.

3. Results and discussions

3.1 Composition characteristics of SP

As summarized in Tables S1–S5,† 179 organic compounds (OCs) from SP were identified in total. Fig. 2 shows the total ion chromatogram of SP, with a retention time of 0–32 minutes selected. As shown in Fig. 3, the OCs can be divided to alkanes, alkenes, arenes, OCOCs and nitrogen-containing organic compounds (NCOCs), and the relative contents are 21.25%, 3.76%, 20.14%, 41.01% and 10.84%, respectively. Among them, the relative content of 69 oxygen-containing compounds was as high as 41.01%, which was consistent with the oxygen content of ISP in proximate analysis.

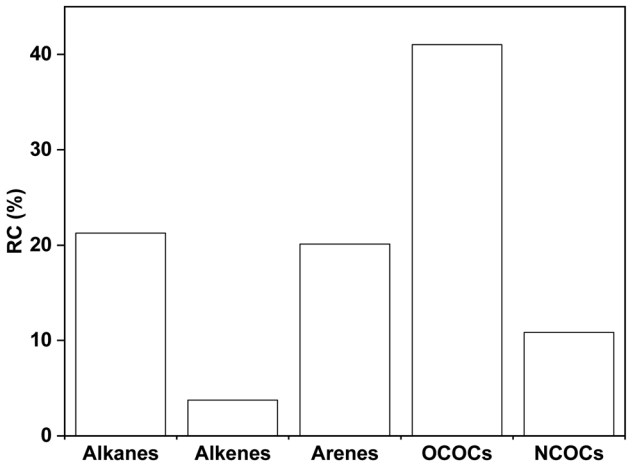

Fig. 3 Distribution of different classes of organic compounds in SP.

In Tables S6–S12,† the OCOCs in SP can be divided into 7 kinds of alcohols, ketones, esters, phenols, aldehydes, ethers and other compounds (OTCs), as shown in Fig. 4, and the relative contents of these OCOCs are 9.92%, 22.84%, 1.15%, 47.85%, 4.15%, 2.86% and 11.21%, respectively.

Therefore, it can be seen from the above results that there are many types and contents of phenolic compounds in SP, and their formation is mainly related to the structure of aromatic ethers and esters in coal. IPA, as a nucleophilic reagent and hydrogen donor reagent, can attack the aromatic ether and aromatic ester bonds in the structure of coal macromolecules, resulting in the formation of phenoxy radicals after their rupture and the formation of more phenolic compounds by combining with the hydrogen providedby IPA. The breakage of the aromatic ether bond during thermal dissolution and its possible pathway for the formation of phenolic compounds are shown in Scheme 1.

3.2 Composition and structure characteristics of ISP

3.2.1 Proximate and ultimate analyses of PLC and ISP. It can be seen from Table 1 that the moisture content of PLC and ISP is low at less than 10%. Meanwhile, the volatile matter and fixed carbon were as high as 46.69% and 53.31% (PLC), 40.12% and 59.88% (ISP), respectively, indicating that PLC and ISP contain abundant organic compounds. The decrease in volatile matter indicates that mild thermal dissolution mainly dissolves

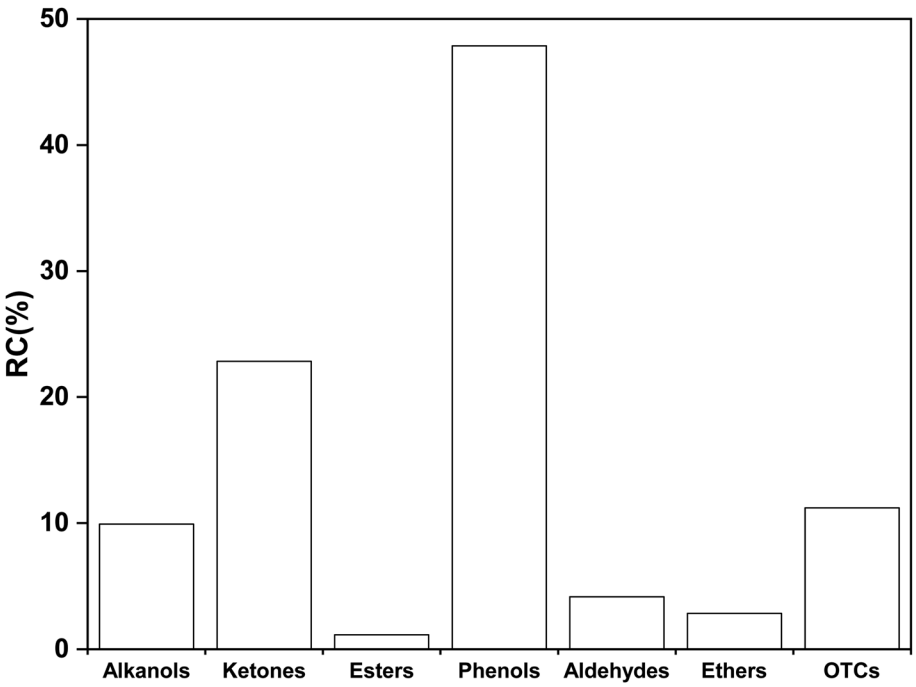

Fig. 4 Distribution of different classes of organic compounds in OCOCs.

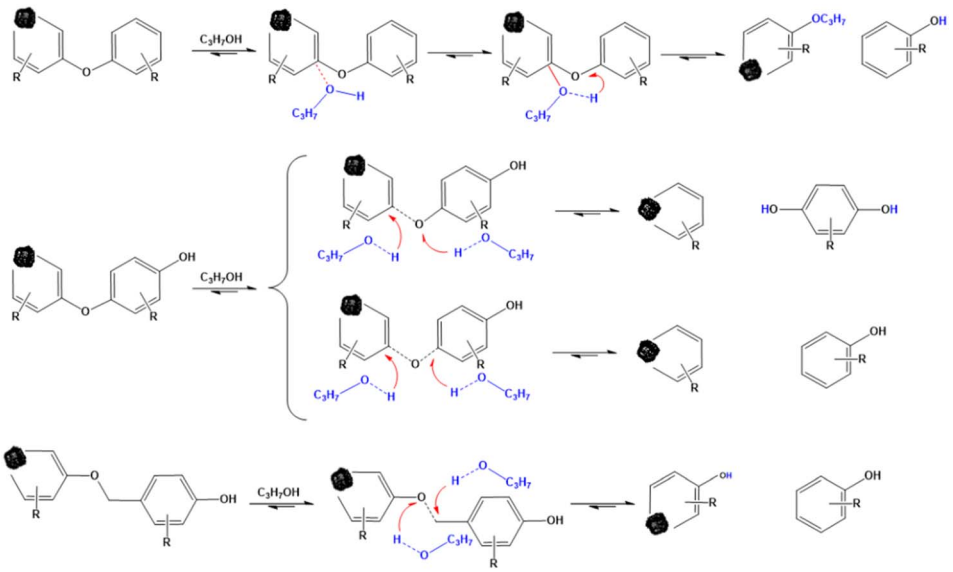

Scheme 1 Possible pathways for the formation of phenols during thermal dissolution.

some light components in low rank coal or small molecules embedded in the macromolecular network structure, without significantly damaging the macromolecular network skeleton structure of the coal.[27]

Literature studies have shown that the main functional groups of organic oxygen in low-rank coals are hydroxyl, carboxyl, carbonyl, and oxygen-containing bridging bonds.[28] The oxygen content in PLC is relatively high (>28.07%); thus, it is speculated that there are more oxygen-containing functional groups in the coal. Meanwhile, the oxygen content in ISP significantly decreased (>23.53%) after thermal dissolution. This may be due to the breaking of carbon oxygen bridge bonds during the thermal dissolution process, resulting in the release of more oxygen-containing compounds. This is consistent with the high content of oxygen-containing molecules in GC-MS and the strong intensity at 1340–1000 cm^{-1} in FTIR.

In addition, the relative content of N and S elements in ISP is significantly higher than that in PLC. This may be due to the cracking reaction of organic matter during coal thermal dissolution, releasing hydrocarbons and oxygen-containing compounds, resulting in a relative increase in the content of N and S elements. It is worth noting that the H/C ratio increased from 0.75 in PLC to 0.78 in ISP, indicating that IPA can dissolve some compounds containing aromatic rings, which may be cyclic or unsaturated molecules.

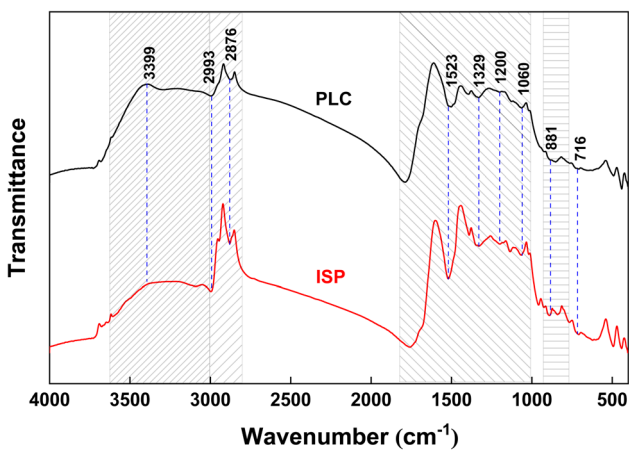

Fig. 5 FTIR spectra of PLC and ISP.

3.2.2 Composition and distribution of functional groups

3.2.2.1 Qualitative analyses. Fig. 5 shows the FTIR spectra of PLC and ISP. The peak intensity of each functional group in PLC and ISP shows significant differences, demonstrating that the thermal dissolution process could affect the macromolecular network of PLC. The main absorption peak in the range of 3600–3100 cm^{-1} is the phenolic hydroxyl group (Ar-OH). It can be clearly seen from the graph that compared with PLC, the absorption peak of ISP at 3399 cm^{-1} is significantly weakened. This indicates that the thermal dissolution process in the presence of alcohol solvent destroys most of the hydrogen bonds in coal, which helps to dissolve the phenolic compounds. The symmetric and asymmetric stretching vibration peaks of alkanes C–H at wavenumbers of 2993 and 2876 cm^{-1} are significantly enhanced, which is related to the abundance of fatty side chains in ISP. On the one hand, thermal dissolution exposes these fat side chains; on the other hand, alcohol solvents might react with certain functional groups to form fatty side chains or bridge bonds. The out-of-plane bending vibration of aromatic C–H is observed in the range of 900–700 cm^{-1}, and the absorption peak intensity of ISP is enhanced, indicating that ISP has more aromatic ring substituents. In addition, carbonates can contribute to changes in intensities and the overall pattern in the spectral regions of 1400–1500 cm^{-1} and 700–830 cm^{-1}. This is consistent with the fact that the ash content of ISP (15.69%) is higher than that of PLC (9.29%) in Table 1.

3.2.2.2 Semi-quantitative analyses. The FTIR spectra can be separated into four regions: hydroxyl band (3600–3000 cm^{-1}),

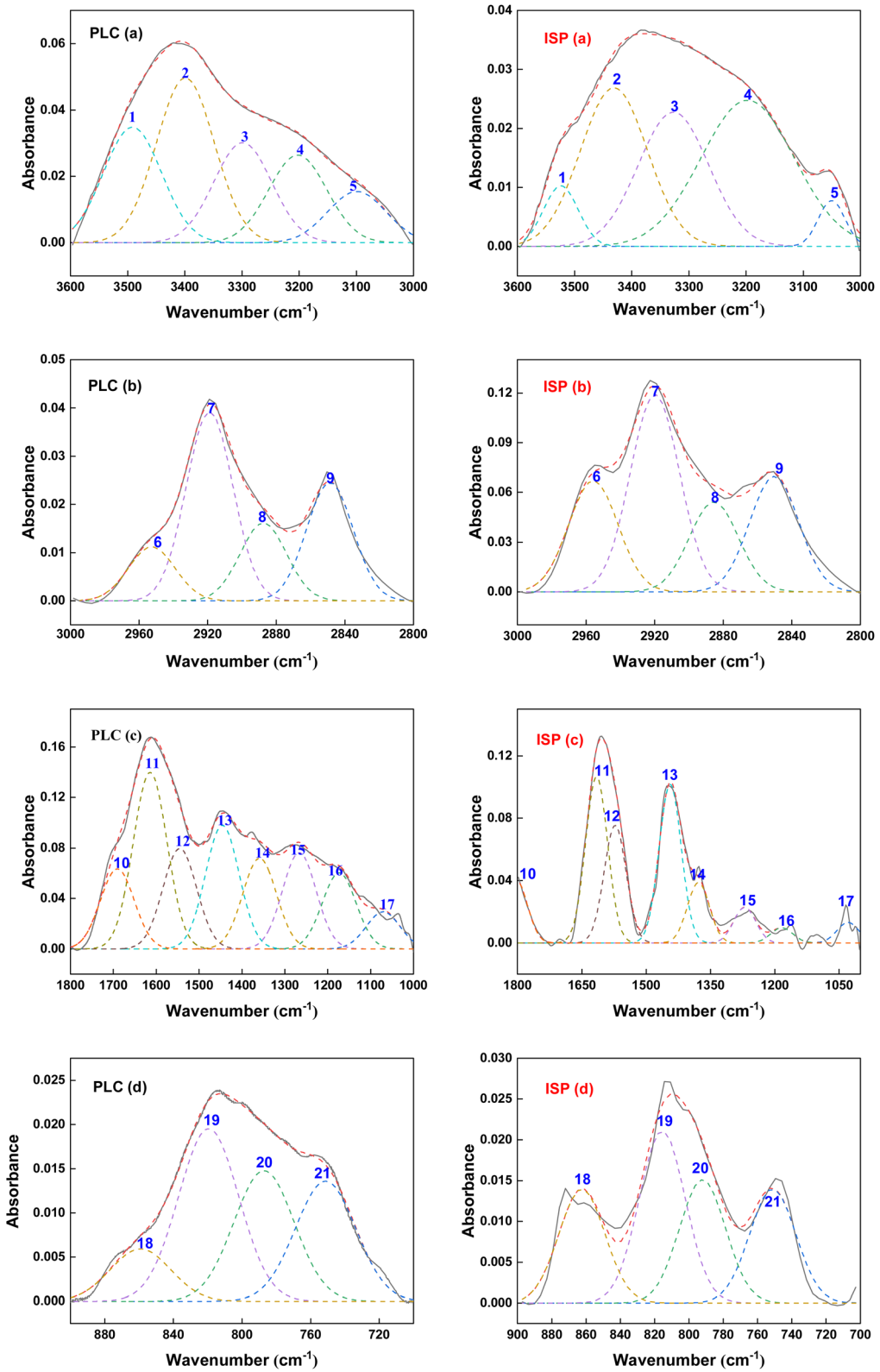

Fig. 6 FTIR peak fitting spectra of PLC (a–d) and ISP (a–d).

aliphatic band (3000–2800 cm^{-1}), oxygen-containing group band (1800–1000 cm^{-1}) and aromatic ring structure band (900–700 cm^{-1}). Peakfit peak fitting software was used to fit the peak curves of the two samples, and the corresponding functional group assignments were provided. Fig. 6 shows the infrared spectrum fitting curves of PLC and ISP, and the

Table 2 Fitting peak attribution of the DTG curve of PLC and ISP[a]

Peak	Assignment	BER (kJ mol^{-1})	PTR (°C)	Area (%) PLC	Area (%) ISP
1	Release of combined water and decarboxylation	<150	<300	9.22	10.47
2	Cracking of weak covalent bonds (>C_{al}–O–, >C_{al}–N< or >C_{al}–S–)	150–230	325–425	8.50	9.40
3	Cracking of strong covalent bonds (>C_{al}–C_{al} < or > C_{al}–H–)	210–230	450–500	52.85	55.89
4	Cleavage of strong covalent bonds (>C_{ar}–C_{al}<, >C_{ar}–O– or > C_{ar}–S–)	300–430	525–600	17.16	13.27
5	CO and CO_2 release from carbonate decomposition	>400	625–710	7.37	7.00
6	Condensation of aromatic rings to release H_2		>725	4.90	3.96

[a] BER: bond energy range; PTR: peak temperature range.

corresponding functional group assignments are shown in Table S13.†

According to Table 2, the peaks at 3600–3000 cm^{-1} were attributed to –OH, and the relative contents of OH–π, OH–OH and OH–N decreased by 16.37%, 3.2% and 6.4%, respectively. The relative contents of OH-ether O and cyclic OH increased by 6.27% and 19.7%, respectively. This shows that the thermal dissolution process breaks most of the hydrogen bonds in the coal, and facilitates the dissolution of phenolic compounds. The absorption peaks at 3000–2800 cm^{-1} were ascribed to aliphatic groups. Compared with PLC, the relative content of the asymmetric stretching vibration of CH_3 in ISP is higher, while other functional groups are reduced, indicating that the fatty hydrocarbon and the compound fatty side chains in ISP are more abundant.

For the vibration absorption peak of oxygen-containing functional groups in the 1800–1030 cm^{-1} region, the relative contents of carboxylic acid C=O in ISP decreased from 10.26% to 5.82%, while the stretching vibration of C–OH in phenols and C–O in esters decreased by 6.49% and 7.27%, respectively. This indicates that a large amount of phenolic, aldehyde, ester, and ether compounds were generated during the thermal dissolution process, which is consistent with the high content of oxygen-containing compounds in GC-MS. The absorption peaks at 900–720 cm^{-1} were ascribed to the aromatic ring structures, and the isolated aromatic hydrogens (1H) and three adjacent hydrogens per ring (3H) in ISP increased by 19.15% and 3.89%, respectively, while two adjacent hydrogens per ring (2H) and four adjacent hydrogens per ring (4H) decreased by 20.18% and 2.86%. It might be concluded that the substitution of aromatic side chains leads to an increase in aliphatic compounds in ISP, resulting in enhanced symmetric and asymmetric stretching vibrations of C–H in alkanes near 2993 cm^{-1} and 2876 cm^{-1}.

3.2.3 Thermal weight loss behavior. Fig. 7 shows the TG-DTG curves of PLC and ISP. The mass loss of PLC (40.69%) is higher than that of ISP (36.36%), which might be derived from the removal of some components by the used solvent. From Fig. 7(right), the maximum weight loss rate peaks of PLC and ISP correspond to temperatures of around 447 °C and 469 °C, respectively, demonstrating that the insoluble macromolecules obtained after the thermal dissolution process present better thermal stability.

To study the information of covalent bonds in PLC and ISP, DTG profiles were fitted to six sub-curves with Peakfit 4.0, and the results are listed in Fig. 8 and Table 2. Peak 1 (30–330 °C) is considered as the emission of bound water and decomposition

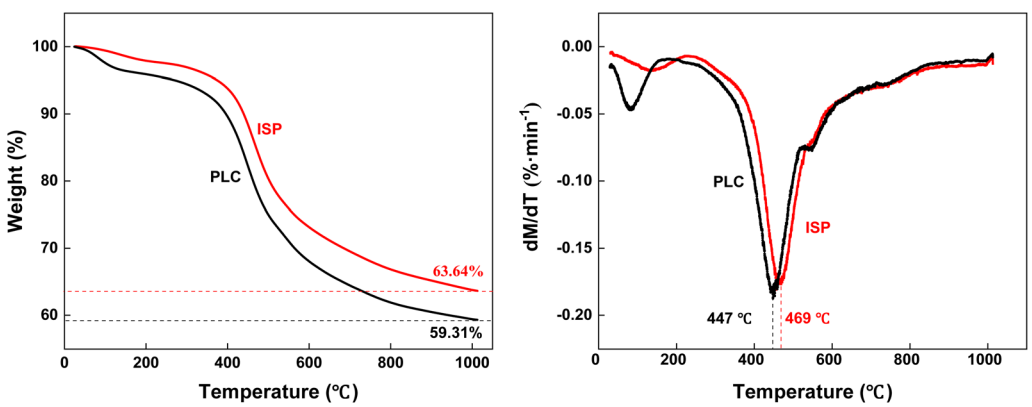

Fig. 7 TG curves (left) and DTG curves (right) of PLC and ISP.

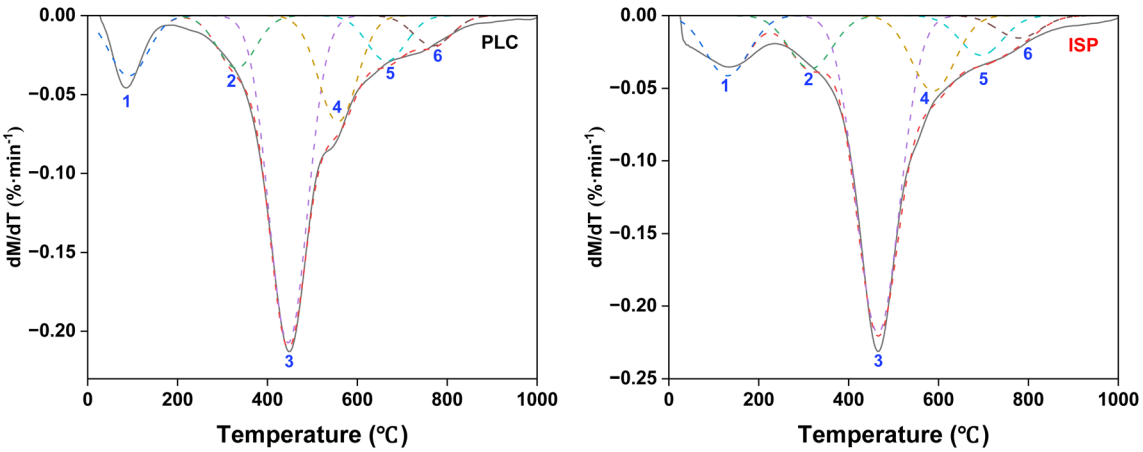

Fig. 8 DTG fitting curves of PLC and ISP.

of carboxy groups. The mass losses of PLC and ISP were 9.22% and 10.47%, respectively, illustrating that thermal dissolution can effectively remove moisture and small molecules in PLC. According to FTIR analyses, the contents of carboxylic compounds in PLC are higher. It is evident that PLC mainly underwent decarboxylation reaction during this stage.

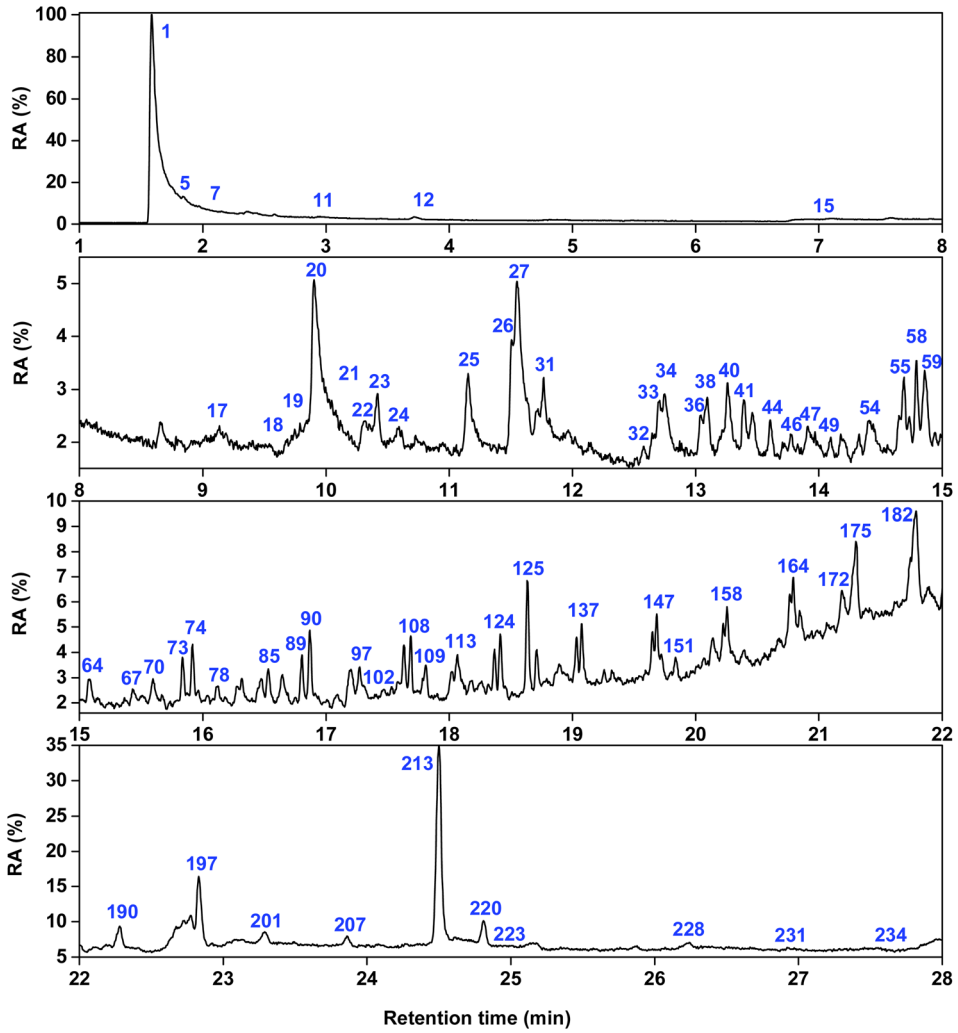

Fig. 9 Total ion chromatograms of PLC.

The temperature range of 330–600 °C mainly corresponded to the thermal-cracking of network organics. In detail, peak 2 can be assigned to the breakage of the >C_{al}–X (X = O–, N< and S<) bond, and the mass losses of PLC and ISP were 8.50% and 9.40%, respectively. According to proximate analyses, the contents of N and S elements in ISP are higher, demonstrating that the samples mainly underwent the cleavage of >C_{al}–N< and >C_{al}–S– bonds, while the contents of the oxygen-containing organic compounds in PLC are higher, and the cleavage of >C_{al}–O– bonds mainly occurs. In addition, peak 3 belongs to the cleavage of strong covalent bonds, such as >C_{al}–C_{al}< and >C_{al}–H–. Meanwhile, the mass losses of PLC and ISP were 52.85% and 55.89%, respectively, illustrating higher contents of aliphatic compounds in ISP, consistent with the FTIR. As the pyrolysis process proceeds, the cleavage of >C_{ar}–O– >C_{ar}–S–, and >C_{ar}–C_{al}< bonds in lignite occurs in the region of peak 4.

Peaks 5 and 6 could be attributed to the last stage of the complex pyrolysis reaction, which is usually thought to be the decomposition of minerals and condensation of polycyclic aromatic compounds, respectively. In this high temperature range, the decomposition of carbonates may produce CO_2.

3.3 Pyrolysis analyses of PLC and ISP

Fig. 9 and 10 show the total ion flow chromatograms of the pyrolysis products at 450 °C of PLC and ISP. The selected retention time range is 1–28 minutes. The detailed analyses results of the products are shown in Tables S14–S18.† Among them, a total of 113 compounds were detected in the PLC pyrolysis products. A total of 101 compounds were detected in the ISP products, which can be divided into 5 categories: alkanes, alkenes, arenes, OCOCs, and NCOCs.

The relative content distributions of the pyrolysis products of PLC and ISP are shown in Fig. 11. Compared with PLC, the contents of alkanes in ISP increased from 30.62% to 49.75%. It can be inferred that alkanes might derive from the emission of low molecules (especially for PLC) and the C_α–C_β bond breakage of aliphatic side chains on the aromatic ring.[4] In addition, 43

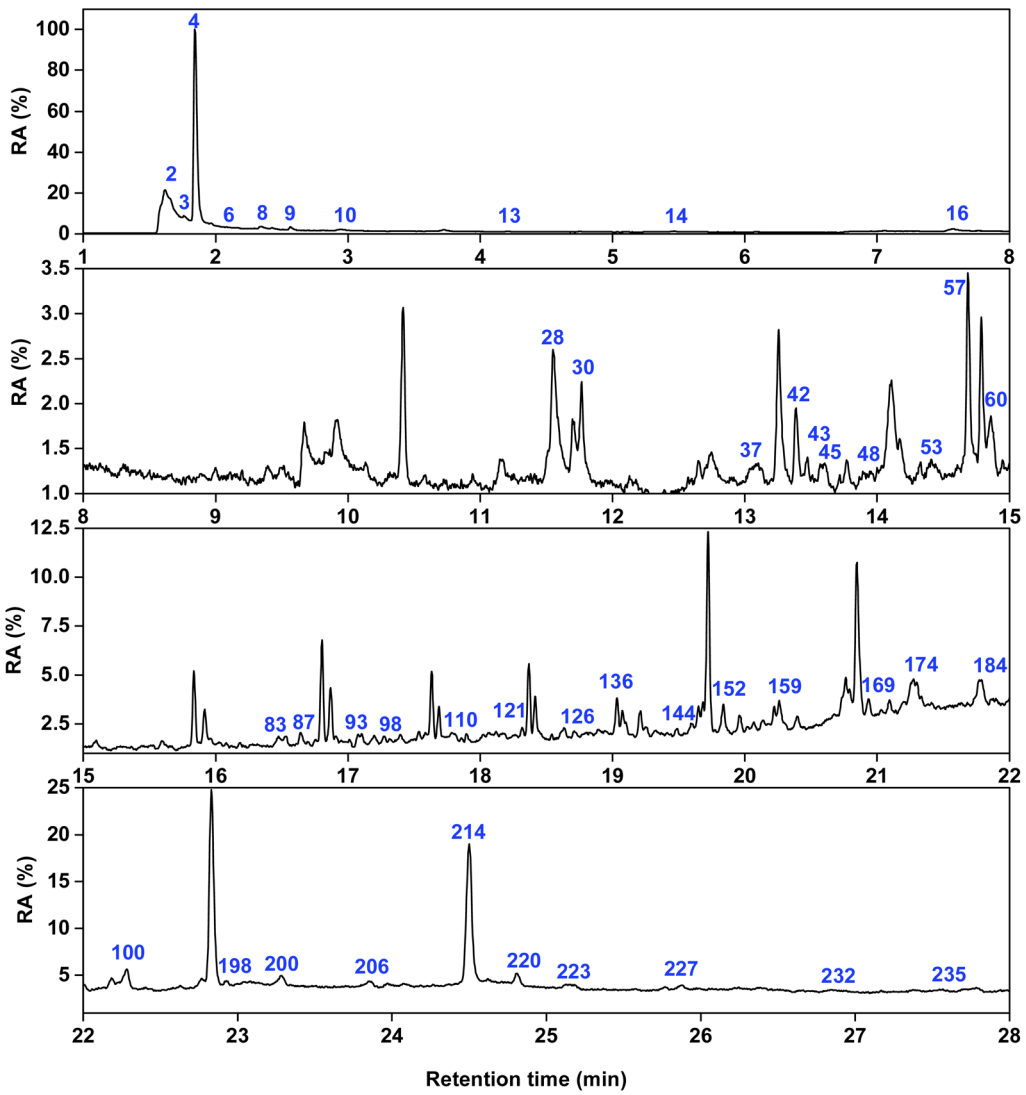

Fig. 10 Total ion chromatograms of ISP.

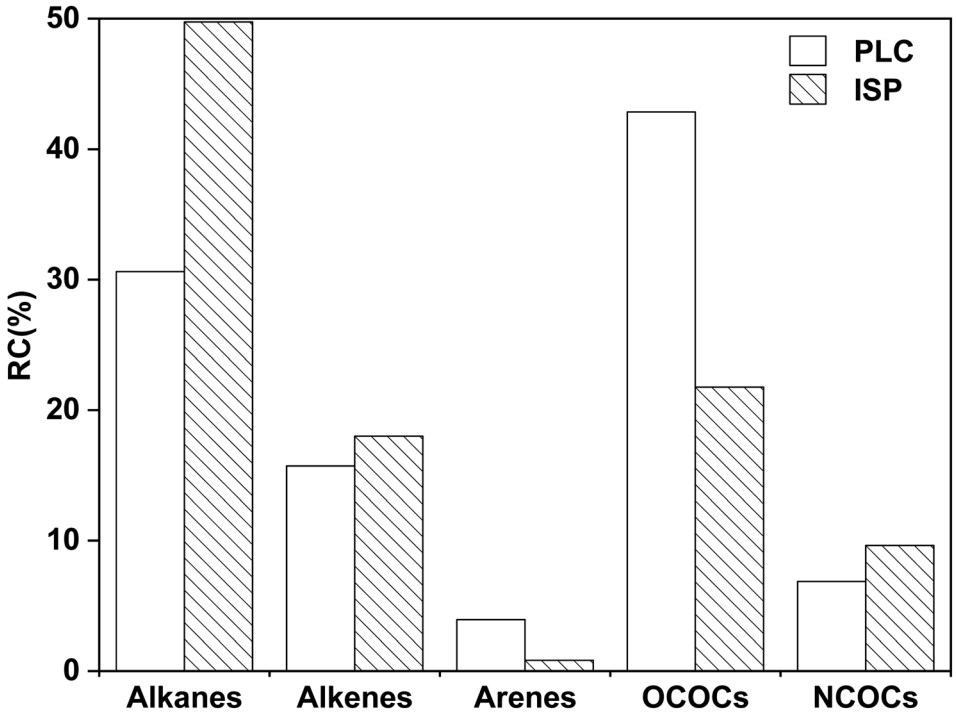

Fig. 11 Distribution of different classes of organic compounds in PLC and ISP.

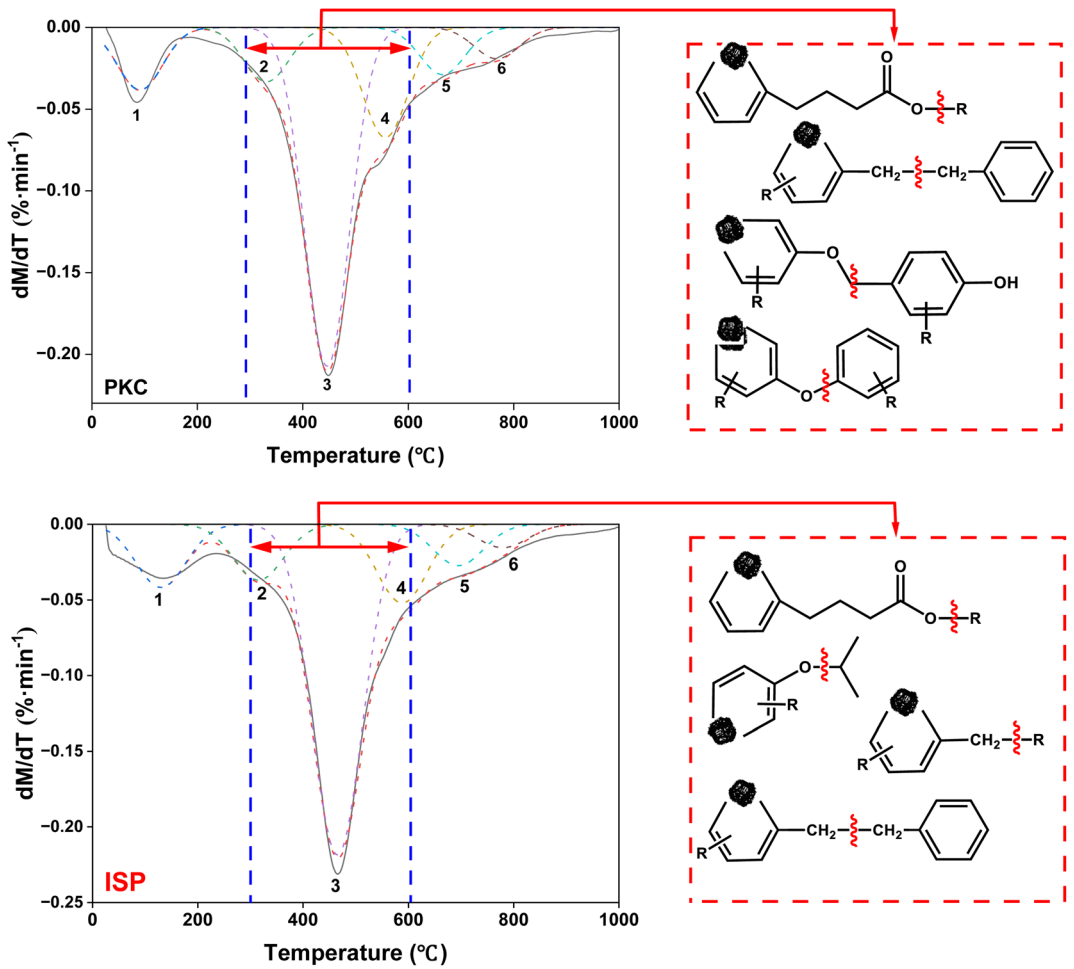

Fig. 12 Possible broken mechanisms of PLC and ISP during fast pyrolysis at 450 °C.

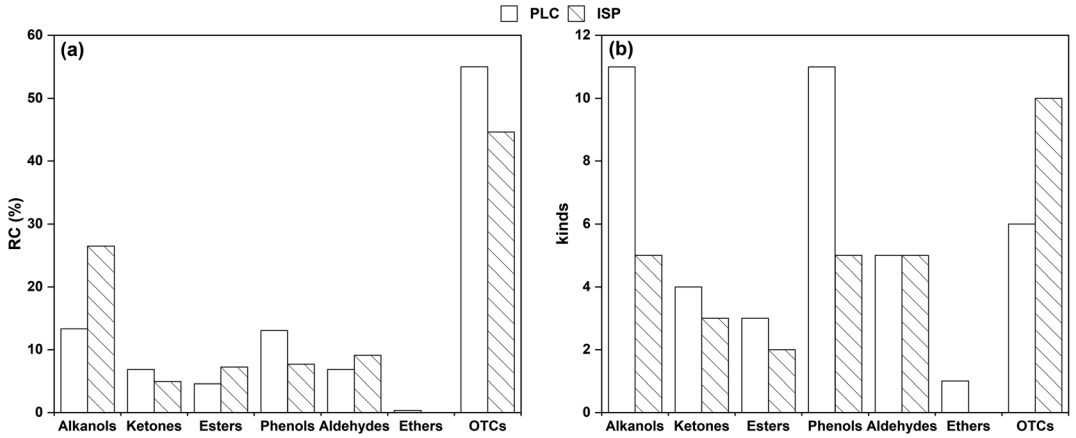

Fig. 13 Distribution of different classes (a) and kinds (b) of OCOCs in PLC and ISP.

kinds of OCOCs were detected in PLC, accounting for 42.87%, and 31 kinds were detected in ISP, with a relative content of 21.78%. This indicates that the IPA thermal dissolution process has partially separated the OCOCs in coal.

Fig. 12 shows the possible broken mechanisms of PLC and ISP during fast pyrolysis at 450 °C. Combined with the DTG analyses, the pyrolysis below 350 °C mainly results in non-covalent bond, and the fatty side chain fracture and the partial oxygen-containing functional group decomposition. Above 350 °C, the covalent bond fracture occurs in PLC, and the cracking of the macromolecular skeleton is intensified. As shown in the figure, PLC generates more aliphatic hydrocarbons and OCOCs through the breaking of chemical bonds, such as –O–R, –CH_2–CH_2–, Ar–C– and Ar–O–. In contrast, there has been an increase in alkane compounds and a relative decrease in oxygen-containing compounds in ISP. This is probably due to the formation of hydrocarbons attributed to the cleavage of fatty side chains, the alkyl bridges connected to aromatic structures, and the aryl alkyl ether bonds.

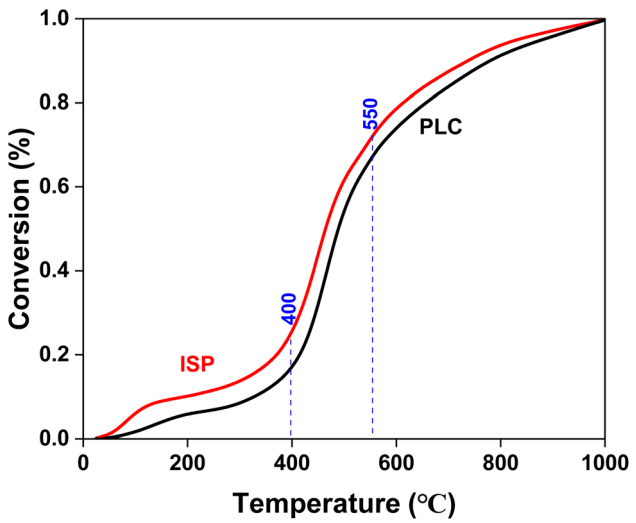

Fig. 14 Pyrolysis conversion-temperature relationship of PLC and ISP.

For further analysis and comparison, the distributions of the different classes (a) and kinds (b) of OCOCs in PLC and ISP are compared, as shown in Tables S19–S25† and Fig. 13. In detail, the content of alcohol increases, while the content of some carboxylic acids decreases. It is speculated that a large number of phenolic compounds are extracted during the thermal dissolution process, resulting in a large number of carboxylic groups in the coal macromolecular groups being exposed and further decomposed into alcohol under heat. It can be seen from Fig. 13b that the types of compounds in both alcohols and phenols decreased, indicating that the oxygen bridge bonds were selectively weakened after thermal dissolution. Furthermore, the broken bonds in the pyrolysis process were more concentrated, resulting in simpler product composition.

The kinetic method can be used for further analysis and comparison.[29–32] As shown in Fig. 14, the pyrolysis conversion-temperature relationship be divided into three stages. Combined with Fig. 12, the maximum weight loss rate peak is mainly located in the second stage (T_{400}–T_{550}), which is the main pyrolysis temperature segment. Based on the Coats-Redfern method, the reaction order (RO) (n = 1, 2 and 3) was used for kinetic analysis of the pyrolysis process. The pyrolysis kinetics fitting diagram is shown in Fig. 15, and the relevant parameters of the pyrolysis kinetics are shown in Table 3. It can be seen that the best fit is n = 3. Compared with PLC (E = 83.15 kJ mol^{-1} and A = 120 161.80 min^{-1}), the activation energy and pre-exponential factor of ISP (72.31 kJ mol^{-1} and 30 092.54 min^{-1}) decreased. It might be inferred that thermal dissolution dissolves small molecular compounds in coal channels, enlarges the pore structure and mass transfer rate, and enables the compounds produced in the pyrolysis process to diffuse to the surface of coal faster.[21] On the other hand, IPA in thermal solution can be used as the hydrogen supply solvent to weaken the oxygen bridge bond in the macromolecular structure of coal, so that it is easier to break during pyrolysis. Therefore, the pyrolysis activity is higher and the pyrolysis process is easier. In addition, the upgraded char may be used as a premium fuel of gasification or combustion.[33]

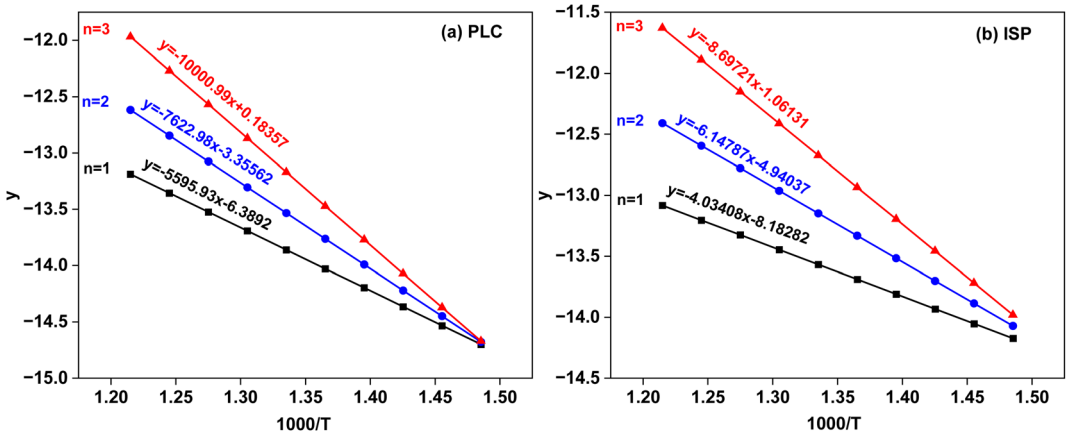

Fig. 15 Pyrolysis kinetics fitting diagram of (a) PLC and (b) ISP.

Table 3 Pyrolysis kinetic parameters of PLC and ISP

Sample	RO	y	R^2	E (kJ mol^{-1})	A (min^{-1})	$2RT/E$
PLC at 400–550 °C						
	1	$-5595.93x - 6.3892$	0.987949	46.52	93.99	0.23
	2	$-7622.98x - 3.35562$	0.99083	63.38	2659.48	0.17
	3	$-10000.99x + 0.18357$	0.99369	83.15	120 161.80	0.13
ISP at 400–550 °C						
	1	$-4034.08x - 8.18282$	0.96126	33.54	11.27	0.43
	2	$-6147.87x - 4.94037$	0.98541	51.11	439.69	0.28
	3	$-8697.21x - 1.06131$	0.99383	72.31	30 092.54	0.20

4. Conclusion

In this, SP and ISP were obtained by IPA thermal dissolution at 300 °C from PLC. The thermal dissolution process mainly dissolves some light components in low-rank coal. The majority of SP is composed of OCOCs (40.83%), mainly comprising phenols, aldehydes, esters, and ethers. The reason for this is that the low-carbon alcohols can effectively break the ether bridge bonds in coal to generate a large number of OCOCs. Both ISP and PLC can detect alkanes, olefins, aromatics, OCOCs, and NCOCs in the products of fast pyrolysis at 450 °C. As a pretreatment method for pyrolysis, thermal dissolution dissolves small molecular compounds in coal channels, enlarges the pore structure and mass transfer rate, and enables the compounds produced in the pyrolysis process to diffuse to the surface of coal faster. On the other hand, IPA can be used as a hydrogen supply solvent to weaken the oxygen bridge bond in the macromolecular structure of coal, so that it is easier to break during pyrolysis. Therefore, the low molecular weight compounds have a significant effect on the low-temperature pyrolysis characteristics of PLC.

Data availability

The data supporting this article have been included as part of the ESI. Data for this article, including DTG, FT-IR, GC/MS and Py-GC/MS, are available at Science Data Bank at **https://www.scidb.cn/en/s/yYrABr**.

Author contributions

Gui-Han Zhao: conceptualization, data curation, writing – original draft. Ya-Ya Ma: writing – review & editing. Yuan Ren: software. Jun Xiao: data curation, software, methodology. Wen-Long Mo: conceptualization, writing – review & editing. Jia Guo: supervision, resources. Xian Yong Wei: project administration, conceptualization. Xing Fan: supervision. Akram Naeem: supervision, resources.

Conflicts of interest

The authors declare that they have no known competing financial interests or personal relationships that could have appeared to influence the work reported in this paper.

Acknowledgements

This work is supported by the special project for regional collaborative innovation of Xinjiang Uyghur Autonomous Region (2022E01057), Tianshan Talents Project of Xinjiang (20243123968), and the science and technology project of Hami (HMKJJH202307).

References

1 B. Q. Lin and M. Y. Raza, Coal and economic development in Pakistan: a necessity of energy source, *Energy*, 2020, **207**, 118244.

2 A. Y. Malik, M. I. Ali, A. Jamal, U. Farooq, N. Khatoon, W. H. Orem, E. P. Barnhart, J. R. SanFilipo, H. He and Z. X. Huang, Coal biomethanation potential of various ranks from Pakistan: a possible alternative energy source, *J. Clean. Product.*, 2020, **255**, 120177.

3 X. Y. Wei, X. Bai, Y. M. Feng, *et al.*, Advances in catalytic hydroconversion of typical heavy carbon resources under mild conditions, *Energy Fuels*, 2023, **37**, 12570–12588.

4 X. B. Hu, H. Xu, W. L. Mo, X. Fan, W. C. Guo, J. Guo, J. M. Niu, H. Y. Mi, Y. Y. Ma and X. Y. Wei, Effect of sequential thermal dissolution on the structure and pyrolysis characteristics of Naomaohu lignite, *Fuel*, 2023, **331**, 125930.

5 C. F. Wang, X. Fan, X. Dong, *et al.*, Insights into the structural characteristics of four thermal dissolution extracts of a subbituminous coal by using higher-energy collisional dissociation, *Fuel*, 2020, **282**, 118844.

6 T. M. Wang, Z. M. Zong, F. J. Liu, *et al.*, Investigation on compositional and structural features of Xianfeng lignite through sequential thermal dissolution, *Fuel Process. Technol.*, 2015, **138**, 125–132.

7 S. Li, Z. M. Zong, J. Liu, F. J. Liu, X. Y. Wei, G. H. Liu and S. K. Wang, Changes in oxygen-functional moieties during sequential thermal dissolution and methanolysis of the extraction residue from Zhaotong lignite, *J. Anal. Appl. Pyrolysis*, 2019, **139**, 40–47.

8 T. Yoshida, C. Li, T. Takanohashi, *et al.*, Effect of extraction condition on "hyper coal" production (2)-effect of polar solvents under hot filtration, *Fuel Process. Technol.*, 2004, **86**(1), 61–72.

9 R. Ashida, M. Morimoto, Y. Makino, *et al.*, Fractionation of brown coal by sequential high temperature solvent extraction, *Fuel*, 2009, **88**(8), 1485–1490.

10 Y. Gao, X. Y. Wei, Y. J. Li, G. H. Liu, Y. H. Kang, X. R. Ma, X. Li, Y. J. Ma, L. Yan, J. J. Bai and Z. M. Zong, Investigation on the structural features of Hanglaiwan subbituminous coal and its residues from solvent extraction and thermal dissolution, *Energy Fuels*, 2020, **34**(12), 15870–15877.

11 F. P. Wu, J. Yan, Y. P. Zhao, *et al.*, Solubility and molecular composition of organic species in low-rank coals during sequential thermal dissolution in cyclohexane and methanol, *Energy Sources, Part A*, 2019, **41**(9), 1132–1139.

12 X. Y. Zhang, R. Y. Wang, F. Y. Ma, *et al.*, Structural characteristics of soluble organic matter in four low-rank coals, *Fuel*, 2020, **267**, 117230.

13 S. Li, Z. M. Zong, S. K. Wang, *et al.*, Compositional features of the extracts from the methanolysis of Xilingol No. 6 lignite, *Fuel*, 2019, **246**, 516–520.

14 Y. Y. Ma, F. Y. Ma, W. L. Mo and Q. Wang, Five-stage sequential extraction of Hefeng coal and direct liquefaction performance of the extraction residue, *Fuel*, 2020, **266**, 117039.

15 Y. C. Zhang, X. Fan, W. Wang, C. F. Wang, G. S. Li, Y. Y. Xu, W. L. Mo, X. Y. Wei and F. Y. Ma, Structural elucidation for soluble organic oxygenated compounds in soft and hard coals using advanced extraction methods, *Fuel*, 2022, **322**, 124069.

16 M. L. Xu, X. Y. Wei, X. Y. Yu, F. J. Liu, Q. C. Wu, S. Li, S. K. Wang, G. H. Liu, Z. Q. Liu, X. H. Guo, Y. Y. Zhang and Z. M. Zong, Insight into molecular compositions of soluble species from sequential thermal dissolution of Liuhuanggou bituminous coal and its extraction residue, *Fuel*, 2019, **253**, 762–771.

17 Y. Y. Zhang, X. Y. Wei, J. H. Lv and Z. M. Zong, Study on the oxygen forms in soluble portions from thermal dissolution and alkanolyses of the extraction residue from Baiyinhua lignite, *Fuel*, 2020, **260**, 116301.

18 L. Zhang, J. Shang, H. Shu, *et al.*, Investigation on the distribution of Yimin lignite pyrolysis products and the stability of its char, *ACS Omega*, 2021, **6**(22), 13953–13961.

19 Y. Li, S. Huang, Y. Wu, *et al.*, Effects of thermal dissolution in different solvents on structural characteristics and pyrolysis behaviors of lignite, *Fuel*, 2019, **241**, 550–557.

20 Y. Liu, L. Yan, P. Lv, *et al.*, Effect of n-hexane extraction on the formation of light aromatics from coal pyrolysis and catalytic upgrading, *J. Energy Inst.*, 2020, **93**(3), 1242–1249.

21 H. Kan, Y. Wang, W. L. Mo, X. Y. Wei, H. Yu Mi, K. J. Ma, M. X. Zhu, W. C. Guo, J. Guo, J. M. Niu and X. Fan, Effect of solvent swelling with different enhancement method on the microstructure and pyrolysis performance of Hefeng subbituminous coal, *Fuel*, 2023, **332**, 126066.

22 Z. F. Wu, X. Y. Wei, W. L. Mo, Y. H. Kang, X. Q. Zhang, X. K. Shan, G. H. Liu and X. Fan, Catalytic hydroconversion of the light residue from Yinggemajianfeng lignite over a solid superacid, *Fuel*, 2022, **310**, 122470.

23 W. L. Mo, Z. F. Wu, X. Q. He, W. J. Qiang, B. Wei, X. Y. Wei, Y. L. Wu, X. Fan and F. Y. Ma, Functional group characteristics and pyrolysis/combustion performance of fly ashes from Karamay oily sludge based on FT-IR and TG-DTG analyses, *Fuel*, 2021, **296**, 120669.

24 Y. Y. Ma, X. Fan, W. L. Mo, G. S. Li, F. Y. Ma and X. Y. Wei, Catalytic hydrogenation and heteroatom removal for isopropanol soluble organic matter of Dongming lignite, *Fuel Process. Technol.*, 2021, **211**, 106589–106595.

25 W. L. Mo, Y. Wang, Y. Y. Ma, Y. J. Peng, X. Fan, Y. L. Wu and X. Y. Wei, Direct liquefaction performance of sub-bituminous coal from Hefeng by solid super acids and

pyrolysis kinetic analysis of the corresponding residue, *J. Anal. Appl. Pyrolysis*, 2021, **159**, 105181.

26 Y. Li, S. Huang, Y. Wu, *et al.*, The roles of the low molecular weight compounds in the low-temperature pyrolysis of low-rank coal, *J. Energy Inst.*, 2019, **92**(2), 203–209.

27 M. L. Xu, X. Y. Wei, X. Y. Yu, F. J. Liu, Q. C. Wu, S. Li, S. K. Wang, G. H. Liu, Z. Q. Liu, X. H. Guo, Y. Y. Zhang and Z. M. Zong, Insights into molecular compositions of soluble species from sequential thermal dissolution of Liuhuanggou bituminous coal and its extraction residue, *Fuel*, 2019, **253**, 762–771.

28 Y. Y. Zhang, X. Y. Wei, J. H. Lu, *et al.*, Characterization of nitrogen-containing aromatics in Baiyinhua lignite and its soluble portions from thermal dissolution, *Chin. J. Chem. Eng.*, 2019, **27**(11), 2783–2787.

29 R. K. Mishra, K. Mohanty and X. Wang, Pyrolysis kinetic behavior and Py-GC-MS analysis of waste dahlia flowers into renewable fuel and value-added chemicals, *Fuel*, 2020, **260**, 116338.

30 R. K. Mishra, Q. Lu and K. Mohanty, Thermal behaviour, kinetics and fast pyrolysis characteristics of cynodon dactylon grass using Py-GC/MS and Py-FTIR analyser, *J. Anal. Appl. Pyrolysis*, 2020, **150**(4), 104887.

31 R. K. Mishra, S. Chinnam and A. Sharma, Catalytic co-pyrolysis behaviour and kinetics study of waste lignocellulosic non-edible seeds and Covid-19 plastic over Al_2O_3 catalyst, *Bioresour. Technol. Rep.*, 2024, **27**, 101899.

32 R. K. Mishra, K. Mohanty and X. Wang, Pyrolysis kinetics behavior and pyrolysate compositions analysis of agriculture waste toward the production of sustainable renewable fuel and chemicals, *Environ. Prog. Sustainable Energy*, 2024, **43**(3), e14357.

33 J. Yan, Z. Bai, P. Hao, *et al.*, Comparative study of low-temperature pyrolysis and solvent treatment on upgrading and hydro-liquefaction of brown coal, *Fuel*, 2017, **199**, 598–605.